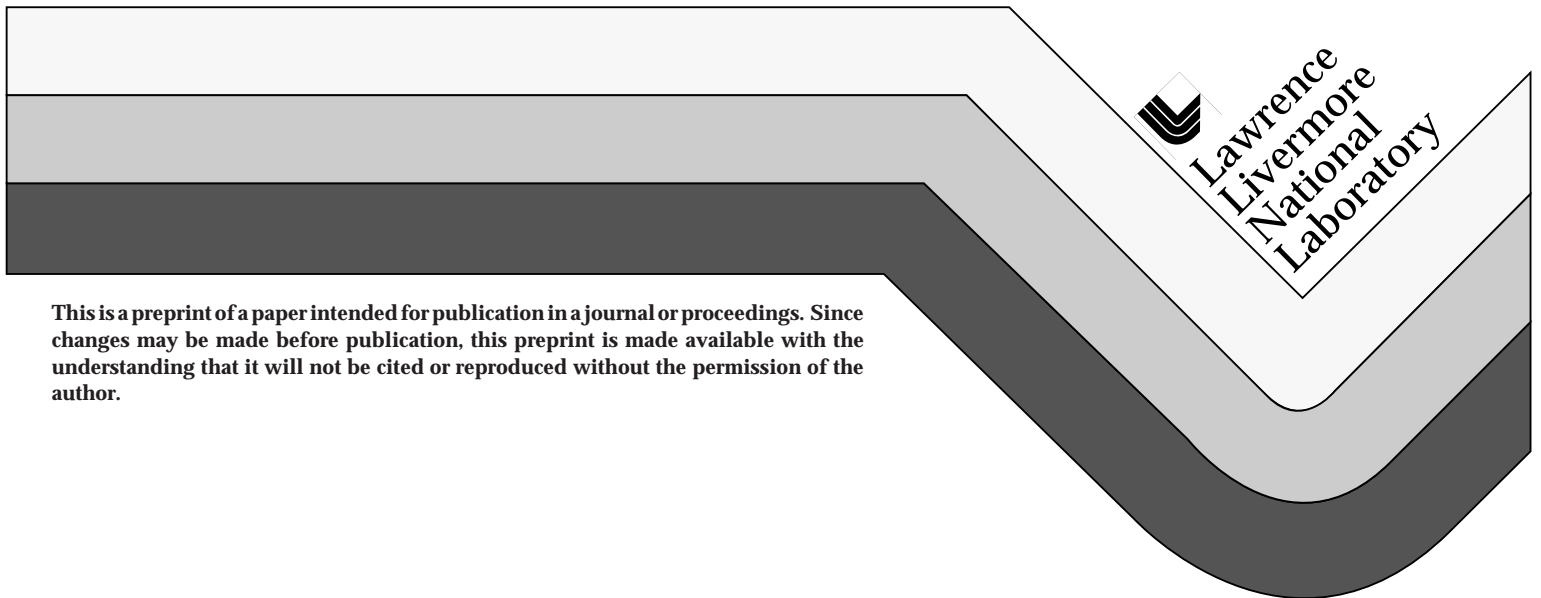


An Experimental Study of the Richtmyer-Meshkov Instability, Including Amplitude and Wavelength Variations

**P. L. Miller, L. M. Logory, T. A. Peyser, D. R. Farley,
S. D. Murray, E. W. Burke, P. E. Stry**

**This paper was prepared for submittal to the
International Symposium on Shock Waves
Great Kappel Island, Queensland, Australia
July 20-25, 1997**

July 1, 1997



This is a preprint of a paper intended for publication in a journal or proceedings. Since changes may be made before publication, this preprint is made available with the understanding that it will not be cited or reproduced without the permission of the author.

DISCLAIMER

This document was prepared as an account of work sponsored by an agency of the United States Government. Neither the United States Government nor the University of California nor any of their employees, makes any warranty, express or implied, or assumes any legal liability or responsibility for the accuracy, completeness, or usefulness of any information, apparatus, product, or process disclosed, or represents that its use would not infringe privately owned rights. Reference herein to any specific commercial product, process, or service by trade name, trademark, manufacturer, or otherwise, does not necessarily constitute or imply its endorsement, recommendation, or favoring by the United States Government or the University of California. The views and opinions of authors expressed herein do not necessarily state or reflect those of the United States Government or the University of California, and shall not be used for advertising or product endorsement purposes.

An experimental study of the Richtmyer-Meshkov instability, including amplitude and wavelength variations

P.L. Miller, L.M. Logory, T.A. Peyser, D.R. Farley, S.D. Murray, E.W. Burke, P.E. Stry

Lawrence Livermore National Laboratory, Livermore, CA 94551, USA

Abstract: We report on results of an experimental study of the Richtmyer-Meshkov instability. The growth of the mixing region in the nonlinear regime is measured for a set of cases in which the amplitude and wavelength of the initial perturbation are varied systematically. The experiments are conducted on the Nova laser facility, and use a Nova hohlraum as a driver source to launch a high-Mach-number shock into a miniature shock tube attached to the hohlraum. The shock tube contains brominated plastic and low-density carbon foam as the two working fluids, with a micro-machined, triangular sawtooth interface between them serving as the initial perturbation. The sawtooth perturbation waveform is dominated by a single mode, and the perturbation amplitudes are chosen to expedite transition into the nonlinear phase of the instability. The shock, upon crossing the perturbation at the interface, instigates the Richtmyer-Meshkov instability. The resulting growth of the mixing region is diagnosed radiographically. Quantitative measurements of the temporal growth of the width of the mixing region are made for six different combinations of amplitude and wavelength, building upon previous results which employed a single amplitude/wavelength combination [Peyser et al. (1995), Miller et al. (1995)]. Data from both experiment and supporting simulations suggest that the nonlinear growth of the mix width admits a logarithmic time dependence. The results also suggest that, properly normalized, the total mixing width grows in a nearly self-similar fashion, with a weak shape dependence.

Key words: Richtmyer-Meshkov, instability, mixing, Nova, laser, experiment

1. Introduction

The present work addresses the behavior of shock-induced instabilities at density interfaces, in the case of very strong driving shocks and for the nonlinear, deeply nonlinear, and turbulent regimes of

the instability development. Use of the Nova facility, located at Lawrence Livermore National Laboratory, provides several advantages in addressing these issues. Nova is capable of generating shocks in the Mach 30 range, in materials of densities on the order of 1 g/cm^3 . The initial perturbations may be imposed by micro-machining the solid materials comprising the interface. These materials vaporize at the start of the experiment or upon the arrival of the shock, obviating the need for membranes or other separation strategies, yet provide us with well-defined and well-known initial conditions. By appropriate selection of the initial perturbation shape we are also able to expedite the transition to the nonlinear regime of interest.

Previous work [Peyser et al. (1995)] has demonstrated that a simple two-phase flow model of the instability growth agrees with the experimental data reasonably well, and that the mixing width increased logarithmically in time. Additional experiments were undertaken to test the applicability of the model, as well as provide fundamental data, by investigating the effects of initial perturbation amplitude, wavelength, and shape on the development of the resulting mixing region. Those additional experiments are reported on here.

2. Description of the experiment

2.1. Experiment setup

The description of these experiments has appeared previously [*e.g.*, Hammel et al. (1993), Peyser et al. (1995)], but is summarized again below for convenience. The experimental configuration is shown in Fig. 1. Eight beams of the Nova laser are used to heat the interior of a cylindrical gold hohlraum to 230 eV. The laser drive beams contain a total energy of 21 kJ in a 1 ns square pulse of $0.35 \mu\text{m}$ wavelength. A cylindrical shock tube made of beryllium (for low x-ray attenuation) is mounted over a hole in the hohlraum. The shock tube contains a brominated polystyrene ab-

lator (density 1.22 g/cm^3) and a low-density carbon resorcinol foam payload (density 0.1 g/cm^3) which act as the two working fluids. A single-mode, rectilinear sawtooth profile is micro-machined into the high-density brominated polystyrene ablator which serves as the perturbation. The shock tube is glued to a gold washer for mounting stability, and the assembled package is then glued to the hohlraum. For more details about the experimental packages, see Louis et al. (1995).

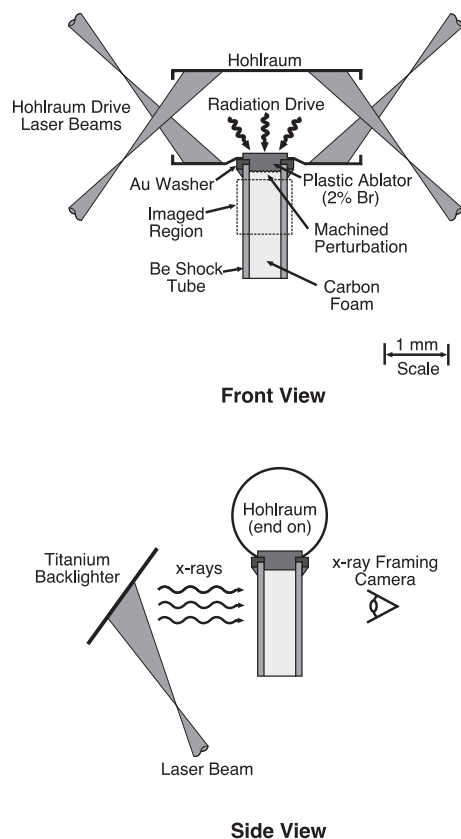


Figure 1. Experiment schematic.

2.2. Experiment sequence

The experiment sequence occurs as follows. Laser irradiation of the interior of the hohlraum produces low-energy x rays which cause a rapid ablation of the surface of the brominated polystyrene exposed to the inside of the hohlraum. The ablation launches a shock into the polystyrene which propagates down the axis of the shock tube. The instantaneous velocity imparted to the interface by the passage of the shock is about $70 \mu\text{m/ns}$. Numerical simulations indicate that at the time the shock is incident on the interface, its Mach number is approximately 30. The passage of the incident shock heats the materials to plasma conditions, at

a temperature of about 10 eV .

The presence of bromine in the polystyrene makes the material radiographically opaque relative to the low-density carbon foam payload. Perturbations consisting of parallel, isosceles, rectilinear sawtooth grooves were machined into the brominated polystyrene with a microlathe. When the shock traverses the interface in the high-to-low density direction, the sawtooth grooves invert, and the instability develops. Two beams of the Nova laser are used to generate x rays, by striking a metal foil, at the appropriate diagnostic time. The shock tube is backlit by the laser-generated x rays, and imaged with an 8x magnification, microchannel-plate-gated x-ray pinhole camera [Budil et al. (1996)], which provides a time-resolved x-ray radiograph of the sample. Fiducial wires provide spatial calibration and reference locations.

The x-ray camera records the image on film which is subsequently scanned and digitized for analysis. Quantitative data is obtained from a vertical lineout of the film exposure levels. The lineout averages the exposure levels over a $100 \mu\text{m}$ wide region at the center of the image. The spatial profile of the x-ray backlighter source is normalized out of the lineout, and the x-ray transmission in the compressed carbon foam behind the shock is normalized to one. Changes in the transmission levels correspond to the uncompressed foam, shock, compressed foam, mix region, and brominated plastic. The width of the mix region is determined by applying a 5 to 95% transmission criteria to the normalized lineout as shown in Fig. 2.

3. Results

We have conducted a series of simulations and experiments in which the temporal evolution of the Richtmyer-Meshkov mixing region was obtained from single-mode triangular perturbations with amplitudes of 5, 10, and $20 \mu\text{m}$, and wavelengths of 11.5, 23, and $46 \mu\text{m}$. These values constitute an amplitude versus wavelength parameter matrix and are shown in Fig. 3. The various amplitudes and wavelengths were chosen to isolate the effects of the initial perturbation geometry and aid in comparisons. Note that perturbations of similar shape are contained within the three diagonals of the matrix. As a complement to the experimental work, simulations of the experiment have been performed using CALE, a two-dimensional arbitrary Lagrangian-Eulerian hydrodynamics code. Simulated radiographs of the developing flowfield were obtained and analyzed in a manner identical to that described for

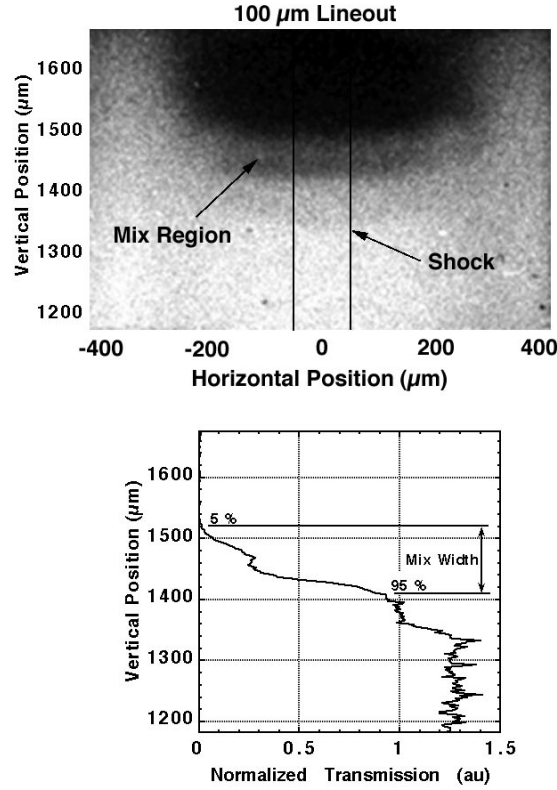


Figure 2. An experimental radiograph of the mix region approximately 8 ns after the shock has crossed the interface. Transitions in the film exposure levels are used to define the mix width.

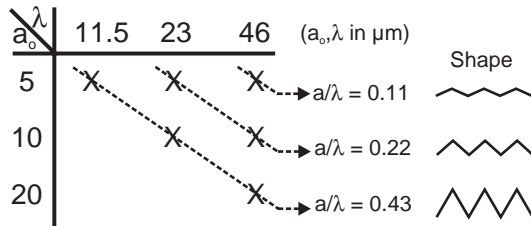


Figure 3. Initial perturbation amplitudes and wavelengths used for both simulations and experiments.

the experimental data. The temporal growth of the mix region obtained from simulations is shown in nondimensionalized form in Fig. 4.

We define the characteristic length-scale of the flow as twice the initial perturbation amplitude, a_0 , and the characteristic velocity as the shock velocity, U_s . A combination of these yields a nondimensional time scale, $U_s/2a_0$, which is the shock transit time across the interface. The time origin is shifted to the time of shock arrival at the first tip of the perturbations, for each of the different initial amplitudes, and then normalized by the shock transit time, yielding the nondimensional time used

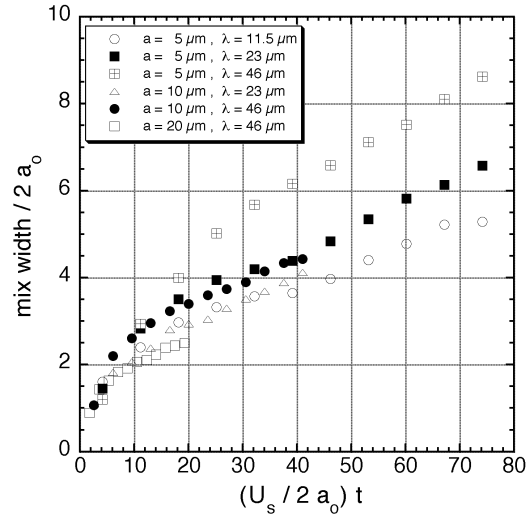


Figure 4. Nondimensionalized temporal width of the mix region obtained from simulations.

in Figs. 4 and 5. In contrast to the incompressible treatment of shock-induced instabilities, the compressible case introduces this natural time scale. As will be seen below, this work validates the use of the initial amplitude as the characteristic length scale. The appropriateness of selecting the shock speed as the velocity scale has not yet been fully tested.

Figure 4 shows that simulations from initial perturbations of the same shape exhibit similarity in these coordinates. The simulations also indicate a weak shape dependence, in which the mix widths obtained from smaller a_0/λ perturbations are larger, in these coordinates. The temporal growth of the mix width for similar shape perturbations are well fit by a logarithmic form (not shown here).

The temporal growth of the mix region measured in the experiment is shown in nondimensionalized form in Fig. 5. Note that data from perturbations of the same shape exhibit similarity in these coordinates. This is in agreement with the results of the simulations shown in Fig. 4. Since previous work [Peyser et al. (1995)] indicated that the mix width admits a logarithmic time dependence, the data for each shape was fit by a three parameter equation of the form $y = m_1 + m_2 \ln(1 + m_3 x)$. The data fits help to further discern the trends for the six different initial perturbations. We find increased mix widths as a_0/λ is decreased, in these coordinates, with the exception of $a_0/\lambda = 0.11$, the most linear initial perturbation. For that case, the mix region extent is nearly equal to that for $a_0/\lambda = 0.22$ up to the nondimensional time of $(U_s/2a_0)t \approx 40$, after

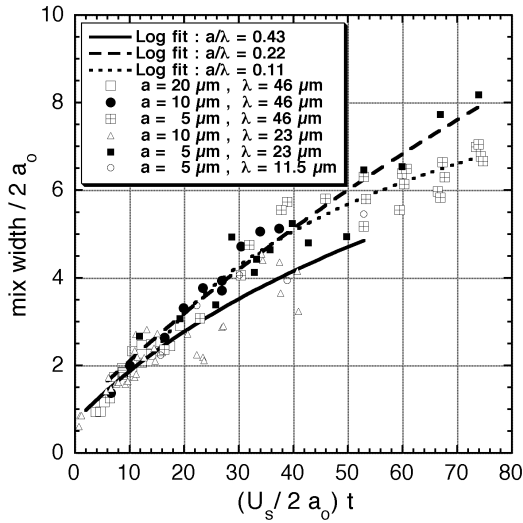


Figure 5. Nondimensionalized temporal width of the mix region obtained from experiments.

which it is less than the $a_0/\lambda = 0.22$ case. It should be noted that the $a_0/\lambda = 0.11$ case is represented by a single amplitude, and the shape is not duplicated elsewhere in the parameter matrix.

Comparing the data displayed in Fig. 5 with the simulations displayed in Fig. 4, we find that the width of the mix region for $a_0/\lambda = 0.43$, for the three different initial amplitudes, is in good agreement for all times. The growth of the mix region for $a_0/\lambda = 0.22$, for two different initial amplitudes, is in good agreement with simulations until approximately $(U_s/2a_0)t \approx 30$, after which the widths grow to be up to 20% larger than that indicated by simulations. Comparison of data with simulations for $a_0/\lambda = 0.11$ indicates the largest disagreement, as can be seen in the comparison of Fig. 4 and Fig. 5. At this time, we have not yet determined the reasons for the discrepancies.

4. Conclusion

We have presented results of an amplitude/wavelength study of the nonlinear Richtmyer-Meshkov growth of predominantly single-mode perturbations, for the case of strong shocks. Six combinations of three amplitudes and three wavelengths were chosen for the study. Data from initial perturbations (with the sawtooth shape) of $a_0/\lambda = 0.43$, for amplitudes of 5, 10, and 20 μm , appear self-similar when both the mixing widths and time are normalized by the initial amplitudes. Similarly, data for the shape with $a_0/\lambda = 0.22$, for amplitudes of 5 and 10 μm collapse in those coordinates. The third shape, of $a_0/\lambda = 0.11$, had

only one amplitude, so collapse for that shape could not be tested.

Comparison between the data from the different shapes indicates that the three cases of $a_0/\lambda = 0.43$ grew less than the two cases of $a_0/\lambda = 0.22$, in the nondimensional coordinates. The single $a_0/\lambda = 0.11$ case had similar mix widths as the $a_0/\lambda = 0.22$ shape until about 40 shock transit times, after which it grew slightly less out to 75 shock transit times. An additional experiment, using $a_0/\lambda = 0.11$, with $a_0 = 2.5 \mu\text{m}$ and $\lambda = 23 \mu\text{m}$, is planned to help clarify the behavior of that shape.

Acknowledgement. The authors would like to thank the individuals who support these experiments, the Nova operations personnel, and those involved in these experiments in the past. Their contributions to the success of this work are gratefully acknowledged. This paper was also presented as part of the Sixth International Workshop on the Physics of Compressible Turbulent Mixing, held in Marseille, France, from 18-21 June, 1997.

This work was performed under the auspices of the U.S. Department of Energy by Lawrence Livermore National Laboratory under Contract No. W-7405-Eng-48.

References

- Budil KS, Perry TS, Bell PM, Hares JD, Miller PL, Peyser TA, Wallace R, Louis H, and Smith DE, The flexible x-ray imager. *Rev. Sci. Instrum.* **67** (2), 1-4 (1996).
- Hammel BA, Griswold D, Landon OL, Perry TS, Remington BA, Miller PL, Peyser TA, and Kilkenny JD, X-ray radiographic measurements of radiation-driven shock and interface motion in solid density material. *Phys. Fluids B* **5** (7), 2259-2264 (1993).
- Louis H, Demiris A, Budil KS, Miller PL, Peyser TA, Stry PE, Wojtowicz DA, and Dimotakis PE, Miniature targets for high-energy density experiments on Nova. *Fusion Tech.* **28** (5), 1769-1882 (1995).
- Miller PL, Peyser TA, Stry PE, and Budil KS, Shock-hydrodynamics experiments on Nova. In: *Proceedings of the 20th International Symposium on Shock Waves*. Pasadena, CA (1995).
- Peyser TA, Miller, PL, Stry, PE, Budil, KS, Burke, EW, Wojtowicz, DA, Griswold, DL, Hammel, BA, Phillion, DW, Measurement of radiation-driven shock-induced mixing from nonlinear initial perturbations. *PRL* **75** (12):2332-2335 (1995).